

# Kinetics and Conversion Monitoring in a RIM Thermoplastic Polyurethane System\*

EDMUND C. STEINLE and FRANK E. CRITCHFIELD, *Union Carbide Corporation, South Charleston, West Virginia 25303* and JOSÉ M. CASTRO and CHRISTOPHER W. MACOSKO, *Department of Chemical Engineering and Materials Science, University of Minnesota, Minneapolis, Minnesota 55455*

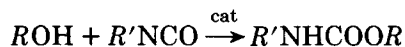
## Synopsis

Kinetic data are reported for the fast polymerization of a thermoplastic polyurethane under conditions similar to that of commercial reaction injection molding (RIM). The components were a 2000 molecular weight polyester polyol, butanediol and 4,4'-diphenylmethane diisocyanate. Three catalysts—dibutyltin dilaurate, phenyl mercuric propionate, and triethylenediamine—as well as uncatalyzed formulations were studied. Kinetic parameters were obtained by numerically fitting adiabatic temperature rise data with both second-order and hyperbolic models. The hyperbolic model gave consistently better fits and is supported by mechanistic studies in the literature. Activation energies compare well to literature values. The uncatalyzed rate was found to be significant. The kinetic parameters obtained by this method are useful measures of catalyst performance in the RIM systems. Moreover, the models provide a convenient way to predict the extent of reaction during the production of parts by the RIM process. The shape of the reaction pathway (extent of reaction versus time) may be important in the development of physical properties of polymers produced by the RIM process. Physical properties for these samples compare favorably to those for a conventionally produced (batch) polyurethane of the same formulation.

## INTRODUCTION

The polyurethanes are a large family of very important block copolymers, probably the oldest and most widely used.<sup>1</sup> The most recent advance in this industry was initiated by the advent of the reaction injection molding (RIM) process. Large polyurethane parts are being reaction injection molded in less than a minute from liquid components. The motivation for growth of these polymerization processing methods is clear: the polymer is formed after the monomer is in the desired shape. Low viscosity monomers or prepolymers can easily fill the mold. Simple low pressure pumping equipment can be used. Great savings in capital equipment, such as molds, clamps, and energy, result.

The primary reaction that occurs during urethane polymerization is



where a hydroxyl group (OH) reacts with an isocyanate group (NCO) in a bulk phase reaction that is usually catalyzed by an organometallic or basic compound. Typical commercial systems involve a polyether-based polyol with functionality greater than 2, a short diol such as 1,4-butanediol (BDO) or ethylene glycol, and

\* Presented in part at the 9th Central Regional American Chemical Society Meeting, October 1977, Charleston, West Virginia.

an isocyanate based on 4,4'-diphenylmethane diisocyanate (MDI). Dibutyltin dilaurate (DBTDL) is often used as the catalyst.<sup>2</sup>

In order to model the RIM molding cycle and to understand how properties develop during the process, it is essential to have some overall reaction kinetic data. Because the RIM-type urethanes react so fast, little kinetic information is presently available.

The present study illustrates a method by which kinetic expressions directly applicable to the RIM process can be obtained. Quantitative data is given for the kinetics of three catalysts. The results can be used to predict extent of reaction in the mold from temperature versus time measurements. These profiles are important for morphology and physical property development in a RIM part.<sup>3</sup>

### Quasiadiabatic Temperature Rise

A large number of methods have been used to monitor the kinetics of polymerization reactions. Kamal<sup>4</sup> and Mussati<sup>5</sup> have given extensive reviews. The most suitable for fast RIM systems seems to be that of following the temperature rise during adiabatic or "quasiadiabatic" reactions.

Macosko and co-workers<sup>6-9</sup> have obtained kinetic expressions from adiabatic polymerization exotherms. They used graphical or linear regression methods for data fitting, with the assumption of constant heat capacity and negligible heat loss during the reaction. The work reported here uses a nonlinear data fitting technique. This method permits the removal of the constant heat capacity assumption. It also allows for the summation of competing reaction pathways and the estimation of heat loss through the walls of the container, to insure a better estimate of the heat of reaction.

To determine the kinetics from a temperature rise, one must be able to relate the extent of reaction to the temperature at any time. To do this, the following assumptions were made: (1) homogeneous, well mixed system at  $t \geq 0$ ; (2) no diffusion effects as molecular weight increases; (3) heat capacity of the reacting mixture modeled by assuming perfect mixing of the heat capacities of the monomers and polymer (Appendix B); (4) constant heat of reaction; (5) rate of heat loss through the walls of the container proportional to the temperature difference between the sample and surroundings; (6) rate of catalyzed reaction proportional to catalyst concentration; (7) constant mechanism throughout the reaction. Both second order and hyperbolic kinetics were tried. The hyperbolic model is preferred because it gives a somewhat better fit to the data and the expression is derived from a generally accepted mechanism for urethane catalysis (Appendix A); (8) Arrhenius temperature dependence of the rate constants

$$k = A \exp[-(E/R)(1/T - 1/T_r)]$$

where  $T_r$  is a reference temperature; and (9) rates of catalyzed and noncatalyzed urethane reactions additive.

With the above-mentioned assumptions, the balance of energy per unit mass becomes the summation of the heat generated by the two reactions minus the heat loss through the walls of the container:

$$C_{pm} \frac{dT}{dt} = H_c R_c + H_n R_n - h^*(T - T_a) \quad (1)$$

Terms are defined in the Nomenclature section. A mole balance for OH groups gives

$$\frac{-dC_{OH}}{dt} = R_c + R_n \quad (2)$$

For the noncatalyzed reaction,  $R_c$  is equal to zero.  $R_c$  and  $R_n$  are given by the expressions developed in Appendix A [eq. (A-5)].

Combining eqs. (1) and (2) with eq. (A-5) and writing the results in terms of extent of reaction  $p$ , we get

$$C_{pm} \frac{dT}{dt} = \frac{H_c K_{c1} \exp[-(E_c/R)(1/T - 1/T_r)] C_c C_{OH_0}^2 (1-p)(r-p)}{1 + K_{c2} C_{OH_0} (1-p)} + \frac{H_n K_{n1} \exp[-(E_n/R)(1/T - 1/T_r)] C_{OH_0}^2 (1-p)(r-p)}{1 + K_{n2} C_{OH_0} (1-p)} - h^*(T - T_a) \quad (3)$$

and

$$\frac{dp}{dt} = \frac{K_{c1} \exp[-(E_c/R)(1/T - 1/T_r)] C_c C_{OH_0} (1-p)(r-p)}{1 + K_{c2} C_{OH_0} (1-p)} + \frac{K_{n1} \exp[-(E_n/R)(1/T - 1/T_r)] C_{OH_0} (1-p)(r-p)}{1 + K_{n2} C_{OH_0} (1-p)} \quad (4)$$

The energy balance after the reaction is essentially complete gives

$$C_{pU} \frac{dT}{dt} = -h^*(T - T_a) \quad (5)$$

Substituting the equation for  $C_{pU}$  (see Appendix B) and integrating using as boundary conditions that at

$$t = t_1, \quad T = T_1$$

and

$$t = t_2, \quad T = T_2$$

we obtain an equation for the modified heat transfer coefficient

$$h^* = \frac{1}{t_2 - t_1} \left[ \alpha_U \ln \left( \frac{T_1 - T_a}{T_2 - T_a} \right) + \beta_U (T_1 - T_2) + \beta_U T_a \ln \left( \frac{T_1 - T_a}{T_2 - T_a} \right) \right] \quad (6)$$

First the parameters for the noncatalyzed reaction  $K_{n1}$ ,  $K_{n2}$ ,  $E_n$ , and  $H_n$  are determined. Then using them as given constants, the parameters for the catalyzed case  $K_{c1}$ ,  $K_{c2}$ ,  $E_c$ , and  $H_c$  are obtained. A nonlinear data fitting technique was used. The program begins at trial values of the adjustable parameters supplied by the operator. These are put in the model and eqs. (3) and (4) are then solved simultaneously, using a Runge-Kutta integration technique. The predicted values for the exotherms are compared against the experimental data to yield a goodness of fit term (root mean deviation squared). Using the Simplex method<sup>10</sup> of steepest ascent optimization, the program selects new trial numbers until no further improvement is noted. The program automatically expands and contracts the step size as it progresses to the optimum. A description of the optimization method and comparison with several other techniques is given by Barneson.<sup>11</sup> The original scheme was proposed by Spendley, Hext, and Humsworth<sup>10</sup> and modified by Nelder and Mead.<sup>12</sup>

Once the kinetic parameters have been obtained, eq. (4) can determine the extent of reaction versus time in the mold, by using the experimental temperature versus time profile. Thus, by positioning a small thermocouple in different parts of the mold the extent of reaction as a function of time and position in the mold can be calculated.

## EXPERIMENTAL

### Materials

Experiments were performed on a thermoplastic polyurethane (TPU) system of type  $A_2, B_2, B'_2$ . The materials are similar to those used in reaction injection molding<sup>1,2</sup> except that the high-molecular-weight polyol was a polyester rather than a polyether as used typically in RIM. Also, the functionality of the system used was two, and all functional groups are expected to be of equal reactivity. Typical RIM systems have a functionality slightly greater than 2.

$A_2$  was 4,4'-diphenylmethane diisocyanate (MDI). The MDI (Multrathane M, Mobay) was purified by heating at 60°C for 2 hr and filtered through a heated filter. The equivalent weight of the isocyanate was measured to be 127.

$B_2$  was 1,4-butanediol.  $B'_2$  was a polycaprolactone diol of 2000 number-average molecular weight (Niax Polyol PCP-0240, Union Carbide Corp.). The equivalent weights of the diols were 45 and 1000, respectively. For each mole of PCP-0240, 4 mole of BDO were used.

Three catalysts were studied: dibutyltin dilaurate (DBTDL, T-12, M and T Chemicals), triethylenediamine (Dabco, Air Products), and phenylmercuric propanoate (PHgP, Methasol 57, Merck Chemical Division, Merck and Co.).

### Procedures

For each catalyst and for the noncatalyzed case, a set of six to eight runs varying in starting temperature, stoichiometry, and catalyst concentration were made, as shown in Table I.

Each run was made using a small laboratory RIM machine of our own design. It is schematically similar to commercial RIM machinery; but uses mechanical stirring instead of impingement mixing. The machine has a flow rate of  $\sim 15$  g/sec and must be solvent flushed immediately after each shot.

The quasiadiabatic experiments were carried out by injecting 50–70 g of reaction mixture from the laboratory RIM machine directly into a double styrene coffee cup. A small copper-constant thermocouple (30-gauge wire) was inserted through the walls of the cup. The fill cycle took 5 sec, after which the cup was covered with a large cork stopper. Temperatures were recorded on a strip chart recorder. Time zero was taken as 2.5 sec, halfway through the fill cycle, about the time the thermocouple was covered by the mixture.

For each run, the temperature was recorded for a period of 15 min. From the first 10 min, ten data points were selected to be used in the nonlinear data fitting procedure. The last 5 min were used to calculate the heat transfer coefficient. Thus since six to eight runs were made, for each case 60–80 data points were used to obtain the kinetic parameters.

To make the plaques for physical testing, an aluminum mold  $5 \times 6 \times 0.125$  in.

TABLE I  
Experimental Design

Case	Starting temperature (°C) $T_0$	Catalyst concentration (PHP) <sup>a</sup> $C$	$r = \frac{C_{NCO_0}}{C_{OH_0}}$
Noncatalyzed	63	—	0.97
	60	—	0.56
	59	—	0.69
	58	—	0.97
	54	—	0.97
	52	—	0.97
DBTDL	67	0.04	1.0
	62	0.02	1.0
	59	0.02	0.6
	59	0.04	0.6
	59	0.04	1.0
	58	0.04	0.6
	56	0.02	1.0
	42	0.02	0.6
Dabco	70	0.28	1.0
	68	0.02	1.0
	63	0.02	1.0
	59	0.02	0.6
	58	0.02	0.6
	56	0.28	0.6
	53	0.28	1.0
	47	0.28	0.6
PHgP	60	0.04	1.0
	60	0.04	0.6
	58	0.04	0.6
	58	0.04	1.0
	57	0.4	1.0
	54	0.4	0.6
	53	0.4	0.6
	53	0.4	1.0

<sup>a</sup> PHP: g of catalyst per 100 g of polyol or % in resin stream.

was used. The mold was preheated to the starting temperature  $T_s$  in an oven. Material at 60°C was injected into the preheated molds with the laboratory RIM machine in approximately 7 sec. The mold was opened after 2 min. For the noncatalytic process, the mold was preheated to 100 or 120°C. After the shot was finished, the mold was put back into the oven for 10 min before demolding. After a delay period of 4–20 hr the plaques were placed in an oven at 100 or 150°C for a post cure period of 1–16 hr.

To follow the in-mold exotherms, two thermocouples were placed in the mold: one at the center and one on the mold surface.

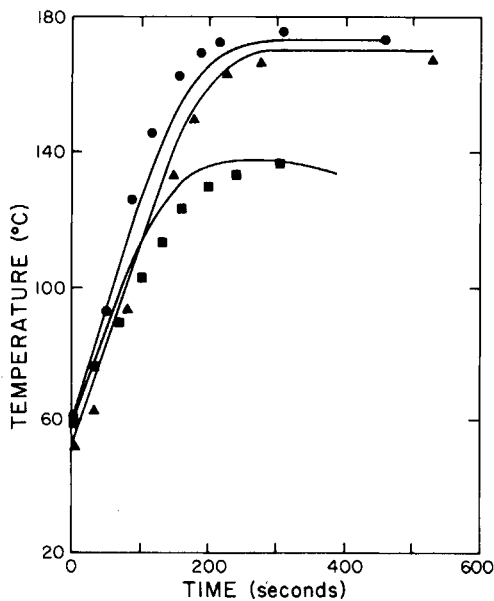


Fig. 1. Temperature rise for runs made with noncatalyzed mixture. The symbols show data points and the lines show model predictions. (●)  $T_0 = 58$ ,  $r = 0.97$ ; (▲)  $T_0 = 52$ ,  $r = 0.97$ ; (■)  $T_0 = 60$ ,  $r = 0.56$ .

## RESULTS AND DISCUSSION

### Kinetics

Figures 1 and 2 show the temperature rise for all six runs made with the non-

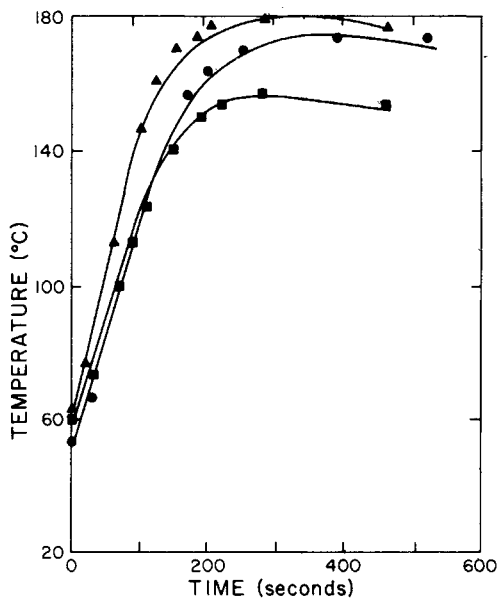


Fig. 2. Noncatalyzed temperature rise data, similar to Fig. 1. (▲)  $T_0 = 63$ ,  $r = 0.97$ ; (●)  $T_0 = 54$ ,  $r = 0.97$ ; (■)  $T_0 = 59$ ,  $r = 0.69$ .

TABLE II  
Estimated Parameters for Hyperbolic Model

	Noncatalyzed	DBTDL	Dabco	PHgP
$K_{c1}$ (g/sec mole php)	19.1	2670	303.	27
$E_c$ (kcal/mole)	5.8	3.3	10.1	15.6
$H_c$ (kcal/mole)	22.1	19.7	19.8	22.1
$K_{c2}$	4.5	0.58	0.02	-0.43

TABLE III  
Effect of Processing Conditions on Physical Properties<sup>a</sup>

Catalyst (% in Polyol)	$T_{mold}$ (°C)	$\eta_{red}$	$E_{flex}$ (24°C)	$E_{flex}$ (70°C)	$\sigma_B$ (25°C) (MPa)	$\epsilon_B$ (%)
Batch Process	140	1.2	190	128	43	480
None	110	0.96	146	95	31	476
0.04 (DBTDL)	60	0.19	160	14	7	38
	82	0.31	75	14	5	64
0.06 (DBTDL)	60	0.82	58	29	25	440
	82	0.90	55	33	29	427
0.4 (PHgP)	82	1.1	72	35	29	423

<sup>a</sup> The properties are average values of several runs. Postcure conditions varied but averaged 125°C for 8 hr. Molar formulation: 1 Polyol/4BD0/5MDI32. Noncatalytic postcured at 125°C for 16 hr.

catalyzed mixture. The symbols show data points and the lines show the model predictions using the best fit parameters listed in Table II. As can be seen, the rate for this noncatalyzed system was significant with the starting temperatures in the 50–60°C range.

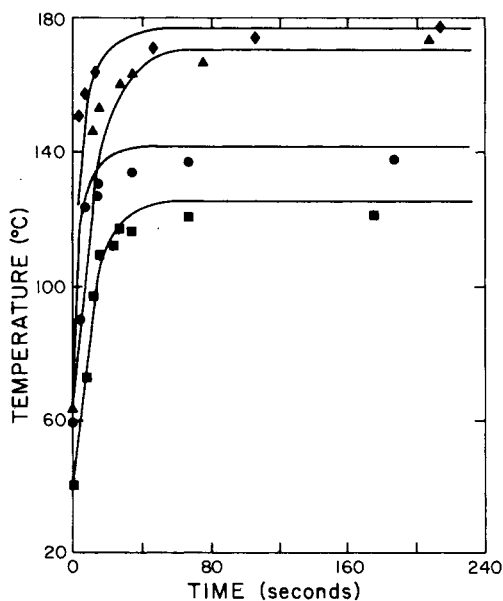


Fig. 3. Temperature rise for four runs of DBTDL catalyzed experiments. The lines show the model predictions using the best fit parameters listed in Table II. ( $\diamond$ )  $T_0 = 67$ ,  $r = 1.0$ ,  $C_c = 0.040$ ; ( $\blacktriangle$ )  $T_0 = 62$ ,  $r = 1.0$ ,  $C_c = 0.020$ ; ( $\bullet$ )  $T_0 = 59$ ,  $r = 0.6$ ,  $C_c = 0.040$ ; ( $\blacksquare$ )  $T_0 = 42$ ,  $r = 0.6$ ,  $C_c = 0.020$ .

Figure 3 shows the data points for four runs of DBTDL catalyzed experiments. The lines show the model predictions using the best fit parameters listed in Table II. Note that the noncatalytic rate was added to the catalytic rate.

As can be seen in Figures 1-3, the model determined for the noncatalyzed and tin catalyzed case gives good predictions of the temperature rise over a series of runs covering wide ranges of catalyst levels, stoichiometry and starting temperatures. Similar results are obtained for the other two catalysts studied. All the adjustable parameters are shown in Table II. The activation energies of DBTDL, Dabco, and PHgP fall in increasing order, in agreement with generally accepted observations. PHgP is one of the highest activation energy catalysts available.

The activation energy could be determined more precisely by making the runs starting at higher and lower temperatures than those used. However, the starting temperature is limited at the low end by the freezing points of the materials and at the high end by the desire to keep the exotherm below 180-200°C to reduce side reactions.

The values of  $K_{c2}$ , the rate constant in the denominator of eq. (3), shown in Table II, are consistent with the activation energies. However, a negative value for the PHgP case shows that the simple hyperbolic mechanism is inappropriate for this high activation energy catalyst.

Finally, the determinations of the heat of reaction presumably should all give the same number, about 25 kcal/equiv.<sup>7,9</sup> The values determined are a measure of the readily available heat of reaction over the temperature range of the exotherms, in the time observed. The fact that the values in Table II are somewhat lower than expected probably reflects lowering of the rate of reaction at high conversion caused by diffusion limitation after phase separation. We have observed that chemical crosslinking also gives drastically slower reactions in the postchemical gel period.

In spite of these limitations, the equations adequately describe the sensible heat generation and extent of reaction as a function of catalyst concentration, stoichiometry, and temperature over the conditions of interest in the RIM molding regime. We have found this approach quite useful, for example, in comparing RIM catalysts, and in calculating conversion profiles through the molding cycle. For example, Figure 4 shows the result of monitoring the tem-

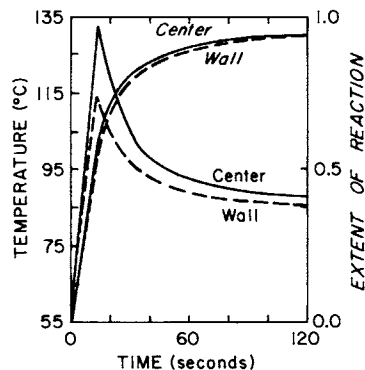


Fig. 4. In-mold exotherms and extent of reaction vs. time, for a system catalyzed with 0.02 wt % DBTDL.



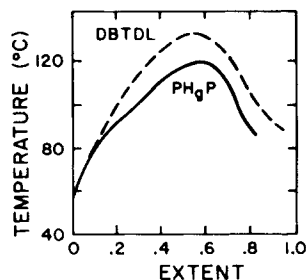


Fig. 5. Comparison of extent of reaction vs. temperature profiles at the mole centerline for a sample catalyzed with DBTDL to one catalyzed with PHgP.

perature rise in the mold for a system catalyzed with 0.02 wt % DBTDL, with initial mold temperature of 71°C. As expected the exotherm at the mold centerline is higher than at the wall due to the low thermal conductivity of the polymer.<sup>6,8</sup> The calculated extents of reaction are also presented. Figure 5 shows the comparison of the extent of reaction versus temperature profiles for a sample catalyzed with DBTDL and one with PHgP.

### Physical Properties

Molecular and mechanical property measurements were done on all samples. The significant trends in reduced solution viscosity, low and high temperature flex modulus, and tensile strength and elongation are summarized in Table III. There was no significant influence of longer cure times and little difference between a 100 and 120°C postcure.

Conventional thermoplastic polyurethane elastomers are typically made by batch polymerization. Total reaction time is 1–2 hr. The product is extruded into pellets and test plaques are compression molded. As indicated in Table III, the resultant polyurethane has a high reduced viscosity corresponding to relatively high molecular weight and high tensile strength and elongation.

These properties can be compared to those for the fast reacted RIM samples. We see that if no catalyst is used, a 110°C mold temperature is required to achieve properties comparable to the batch polymer. Mold temperature for catalyzed samples must be kept lower to prevent decomposition due to the very high exotherm. Typically RIM molds are kept at 60–80°C. We see that with 0.04 wt % of DBTDL catalyst a weak, low molecular weight (low  $\eta_{red}$ ) is produced; however, with 0.06 wt %, typical of commercial formulations, high molecular weight and elongation are achieved. Tensile strength is about 60% of the batch polymer. The low temperature flex moduli are similar but there is a significant

TABLE IV  
Heat Capacity Data<sup>a</sup>

Compound	$\alpha$	$\beta$
Urethane	0.22	0.000756
Extender	0.0231	0.001738
Polyol	0.2623	0.000605
Isocyanate	0.1342	0.000710

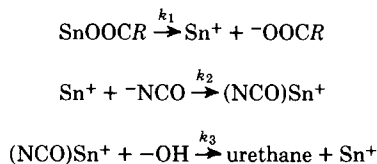
<sup>a</sup>  $C_p = \alpha + \beta T$ , where  $T$  in K to obtain  $C_p$  in cal/g K.

drop at high temperature, which suggests less perfect phase separation in the RIM sample. This can be caused by two different effects: thermal history and hard segment sequence distribution. Both effects can arise as a result of the temperature changes with time and position in the mold. Different portions of the sample have different reaction paths and different annealing conditions.<sup>3</sup> Mixing may also influence segment distribution. Further studies should be done to determine which is dominant with the goal of finding the optimum properties possible by the RIM process.

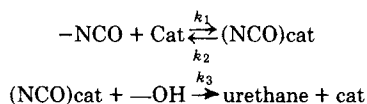
Table III and this discussion have emphasized differences between RIM and conventional batch thermoplastic urethanes of the same formulation. What is remarkable is that their properties are so similar. To produce a plaque from a batch TPU requires two high temperature cycles and considerable process time. The same components via RIM can form a plaque in 3 min with a 60°C mold and a modest postcure.

### APPENDIX A: KINETIC MECHANISM

In this work we have attempted to use a more realistic kinetic model than previously to fit adiabatic rise data.<sup>6,7</sup> Richter and Macosko<sup>9</sup> have shown that the following mechanism fits their kinetic data on a simple MDI plus polyester urethane system catalyzed with DBTDL:



Lipatova<sup>13</sup> has proposed a simpler mechanism for the catalyzed urethane reaction. The first two steps of the Richter and Macosko mechanism become one pseudo-steady-state step



which gives

$$-\frac{dC_{\text{OH}}}{dt} = \frac{dC_U}{dt} = \frac{k_1(k_3/k_2)C_{\text{OH}}C_{\text{NCO}}C_c}{1 + (k_3/k_2)C_{\text{OH}}} \quad (\text{A-1})$$

This is probably the simplest two step mechanism possible and most amenable to numerical fitting of data. In the first step, the catalyst (cat) reacts with an isocyanate group ( $\text{-NCO}$ ) to form the activated complex  $[(\text{NCO})\text{cat}]$ . In the second step the activated complex undergoes reaction with a hydroxyl group ( $\text{-OH}$ ) to form the urethane product and release the catalyst. Assuming an Arrhenius temperature dependence of the rate constants we get

$$\frac{k_1 k_3}{k_2} = \frac{A_1 A_3}{A_2} \exp\left[-\frac{E_1 + E_3 - E_2}{R} \left(\frac{1}{T} - \frac{1}{T_r}\right)\right] \quad (\text{A-2})$$

and

$$\frac{k_3}{k_2} = \frac{A_3}{A_2} \exp\left[-\frac{E_3 - E_2}{R} \left(\frac{1}{T} - \frac{1}{T_r}\right)\right] \quad (\text{A-3})$$

We will further assume that

$$E_3 = E_2$$

to obtain

$$-\frac{dC_{\text{OH}}}{dt} = \frac{dC_U}{dt} = \frac{K_{c1} \exp[-(E_c/R)(1/T - 1/T_r)] C_c C_{\text{OH}} C_{\text{NCO}}}{1 + K_{c2} C_{\text{OH}}} \quad (\text{A-4})$$

where

$$K_{c1} = A_1 A_3 / A_2$$

and

$$K_{c2} = A_3 / A_2$$

Equation (A-4), in terms of the extent of reaction, becomes

$$\frac{dp}{dt} = \frac{K_{c1} \exp[-(E_c/R)(1/T - 1/T_r)] C_c C_{OH_0} (1-p)(r-p)}{1 + K_{c2} C_{OH_0} (1-p)} \quad (\text{A-5})$$

When eq. (A-5) is used for the "noncatalyzed" case,  $C_c$  is taken as unity and  $K_{c1} = K_{n1}$ , etc.

## APPENDIX B: HEAT CAPACITY OF THE MIXTURE

The heat capacities of the monomers and polymer were experimentally determined as a function of temperature using a differential scanning calorimeter (Perkin-Elmer, DSC II), showed generally a linear dependence on temperature<sup>7,14</sup>

$$C_p = \alpha + \beta T \quad (\text{B-1})$$

The values of  $\alpha$  and  $\beta$  for the monomers and polymers are given in Table IV.

The heat capacity of the mixture was calculated by assuming simple weight average additivity of the heat capacities of the monomers and polymer.<sup>15</sup> For the resin mixture of extender and polyol, we have

$$C_{pOH} = C_{pOH\epsilon} \epsilon + C_{pOHp}(1 - \epsilon) \quad (\text{B-2})$$

where

$$\epsilon = \text{g extender/g resin}$$

thus

$$C_{pOH} = [\alpha_{OH\epsilon} \epsilon + \alpha_{OHp}(1 - \epsilon)] + [\beta_{OH\epsilon} \epsilon + \beta_{OHp}(1 - \epsilon)] T \quad (\text{B-3})$$

Defining

$$\alpha_{OH} = \alpha_{OH\epsilon} \epsilon + \alpha_{OHp}(1 - \epsilon) \quad (\text{B-4})$$

$$\beta_{OH} = \beta_{OH\epsilon} \epsilon + \beta_{OHp}(1 - \epsilon) \quad (\text{B-5})$$

we have

$$C_{pOH} = \alpha_{OH} + \beta_{OH} T \quad (\text{B-6})$$

Then, the heat capacity of the mixture becomes

$$C_{pm} = C_{pOH} w_{OH} + C_{pNCO} w_{NCO} + C_{pU}(1 - w_{OH} - w_{NCO}) \quad (\text{B-7})$$

where  $w_{OH}$  is the weight fraction of resin equal to  $C_{OH_0}(1-p)E_{qOH}$  and  $w_{NCO}$  is the weight fraction of isocyanate equal to  $C_{OH_0}(r-p)E_{qNCO}$ . Substitution of the expressions for  $C_p$  into the above equation gives

$$C_{pm} = [(\alpha_{OH} - \alpha_U)w_{OH} + (\alpha_{NCO} - \alpha_U)w_{NCO} + \alpha_U] + [(\beta_{OH} - \beta_U)w_{OH} + (\beta_{NCO} - \beta_U)w_{NCO} + \beta_U] T \quad (\text{B-8})$$

Equation (B-8) is the heat capacity of the mixture as a function of extent of reaction and temperature.

## NOMENCLATURE

- $A$  area available for heat transfer ( $\text{cm}^2$ )  
 $A_c$  kinetic rate constant at  $T_r$  for the catalyzed reaction in second order model

$A_n$	kinetic rate constant at $T_r$ for the noncatalyzed reaction in the second order model $\left(\frac{\text{mole OH}}{\text{g mixture}}\right)^{-1} \left(\frac{\text{g catalyst}}{\text{g mixture}}\right)^{-1} \text{sec}^{-1}$
$C_{pm}$	heat capacity at constant pressure of the reacting mixture (cal/g K) = $\alpha + \beta T$ (K) [eq. (12)]
$C_{pOH}$	heat capacity at constant pressure of the resin (polyol + extender) (cal/g K) = $\alpha_{OH} + \beta_{OHT}$
$C_{pU}$	heat capacity at constant pressure of the urethane (cal/g K) = $\alpha_U + \beta_U T$
$C_{pOHp}$	heat capacity at constant pressure of the polyol (cal/g K) = $\alpha_{OHp} + \beta_{OHp} T$
$C_{pOHe}$	heat capacity at constant pressure of the extender (cal/g K) = $\alpha_{OHe} + \beta_{OHe} T$
$C_{pNCO}$	heat capacity at constant pressure of the isocyanate (cal/g K) = $\alpha_{NCO} + \beta_{NCO} T$
$C_{OH}$	concentration of OH groups at time $t$ (mole OH/g mixture) = $C_{OH_0}(1 - p)$
$C_{NCO}$	concentration of NCO groups at time $t$ (mole NCO/g mixture) = $C_{OH_0}(r - p)$
$C_{OH_0}$	initial concentration of OH groups (mole OH/g mixture) = $1/(E_{qOH} + rE_{qNCO})$
$C_{NCO_0}$	initial concentration of NCO groups (mole NCO/g mixture)
$C_c$	catalyst concentration: $\left(\frac{\text{g of catalyst}}{\text{g of mixture}}\right) = \frac{\text{PHP}}{100 + x^*100}$
$E_{qOH}$	equivalent weight of the resin (g resin/1 mole OH)
$E_{qNCO}$	equivalent weight of isocyanate (g isocyanate/1 mole NCO)
$E_{qU} = E_{qOH} + E_{qNCO}$	equivalent weight of the polymer (g of polymer/1 mole of urethane)
$E_c$	activation energy of the catalyzed reaction (cal/mole OH)
$E_n$	activation energy of the noncatalyzed reaction (cal/mole OH)
$H_c$	heat evolved during the catalyzed reaction (cal/mole OH)
$H_n$	heat evolved during the noncatalyzed reaction (cal/mole OH)
$h$	heat transfer coefficient (cal/K cm <sup>2</sup> sec)
$h^*$	$\frac{hA}{M}$ (cal/g sec K)
$K_{c1}$	constant appearing in the numerator for the hyperbolic type kinetics [eq. (A-6)] in the catalyzed reaction $\left(\frac{\text{mole OH}}{\text{g mixture}} \frac{\text{g catalyst}}{\text{g mixture}} \text{sec}\right)^{-1}$
$K_{c2}$	constant appearing in the denominator for the hyperbolic type kinetics [eq. (A-6)] in the catalyzed reaction (mole OH) g mixture <sup>-1</sup>
$K_{n1}$	constant appearing in the numerator for the hyperbolic type kinetics [eq. (A-6)] in the noncatalyzed reaction $\left(\frac{\text{mole OH}}{\text{g}} \text{sec}\right)^{-1}$
$K_{n2}$	constant appearing in the denominator for the hyperbolic type kinetics [eq. (A-6)] in the noncatalyzed reaction (mole OH) g mixture <sup>-1</sup>
$M$	mass of the reacting mixture (g)
$p$	extent of reaction in terms of OH groups $(C_{OH_0} - C_{OH})/C_{OH_0}$ (dimensionless)
$r$	$C_{NCO_0}/C_{OH_0}$ (dimensionless)
$R_c$	catalyzed reaction rate (mole OH/g sec)
$R_n$	noncatalyzed reaction rate (mole OH/g sec)
$t$	time (sec)
$T$	absolute temperature (K)
$T_a$	ambient temperature (K)
$T_r$	reference temperature for the kinetic rate, 373 K
$T_2$	temperature upper limit used in the determination of the heat transfer coefficient [eq. (6)] (K)
$T_1$	temperature lower limit used in the determination of the heat transfer coefficient [eq. (6)] (K)
$T_0$	initial material temperature (K)
$t_1$	time lower limit used in the determination of the heat transfer coefficient [eq. (6)] (sec)
$t_2$	time upper limit used in the determination of the heat transfer coefficient [eq. (6)] (sec)

$w_{\text{NCO}}$	weight fraction of isocyanate (g isocyanate/g mixture) = $C_{\text{OH}_0}(1-p)E_{q\text{NCO}}$
$w_{\text{OH}}$	weight fraction of resin (g resin/g mixture) = $C_{\text{OH}_0}(1-p)E_{q\text{OH}}$
$x$	$r E_{q\text{NCO}}/E_{q\text{OH}}$
$\alpha$	constant appearing in the heat capacity expression (cal/g K)
$\beta$	constant appearing in the heat capacity expression (cal/g K <sup>2</sup> )
$\epsilon$	weight fraction of extender on the polyol stream (g extender/g resin)

## References

1. A. Noshay and J. E. McGrath, *Block Copolymers Overview and Critical Survey*, Academic, New York, 1976.
2. S. H. Metzger and D. S. Prepelka, in *Advances in Urethane Science and Technology*, Vol. 4, K. C. Frisch and S. C. Reigan, Eds., Technomic, Westport, CT, 1976.
3. M. V. Tirrell, L. J. Lee, and C. W. Macosko, in *Conversion and Composition Profile in Polyurethane Reaction Molding*, Am. Chem. Soc. Symp. Ser., J. N. Henderson and T. C. Bouton, Eds., American Chemical Society, Washington, D.C., 1979, Vol. 104, p. 149.
4. M. R. Kamal, *Polym. Eng. Sci.*, **14**, 231 (1974).
5. F. G. Mussatti, Ph.D. thesis, University of Minnesota, 1975.
6. E. Broyer and C. W. Macosko, *AIChE J.*, **22**, 276 (1976).
7. S. D. Lipshitz and C. W. Macosko, *J. Appl. Polym. Sci.*, **21**, 2089 (1977).
8. E. Broyer, C. W. Macosko, F. E. Critchfield, and L. F. Lawler, *Polym. Eng. Sci.*, **18**, (1978).
9. E. B. Richter and C. W. Macosko, *Polym. Eng. Sci.*, **18**, 1012 (1978).
10. W. Spendley, G. R. Hext, and F. R. Himsworth, *Technometrics*, **4**(4), 441 (1962).
11. R. A. Bameson, N. F. Brannoek, J. G. Moore, and C. Morris, *Chem. Eng.*, **77**(16), 132 (1970).
12. A. J. Nelder and R. Mead, *Comput. J.*, **7**, 309 (1965).
13. T. E. Lipatova, in *Advances in Urethane Science and Technology*, Vol. 4, K. C. Frisch and S. C. Reigan, Eds. Technomic, Westport, CT, 1976.
14. H. Van Krevelan, *Polymer Properties*, 2nd ed., North-Holland, Amsterdam, 1977.
15. J. M. Smith and H. C. Van Ness, *Introduction to Chemical Engineering Thermodynamics*, 2nd ed., McGraw-Hill, New York, 1959.

Received December 12, 1979

Accepted March 13, 1980